Hydrogen bond breakage: the microscopic view.

Tony McCaffery

Department of Chemistry

University of Sussex

Hanna Reisler + coworkers. USC

Marisian Pritchard Sussex

H-bonds found in many environments..

Formed when an H-atom lies
between two electronegative atoms,
to one of which it is covalently bound.

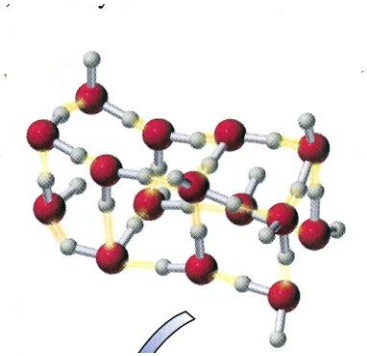

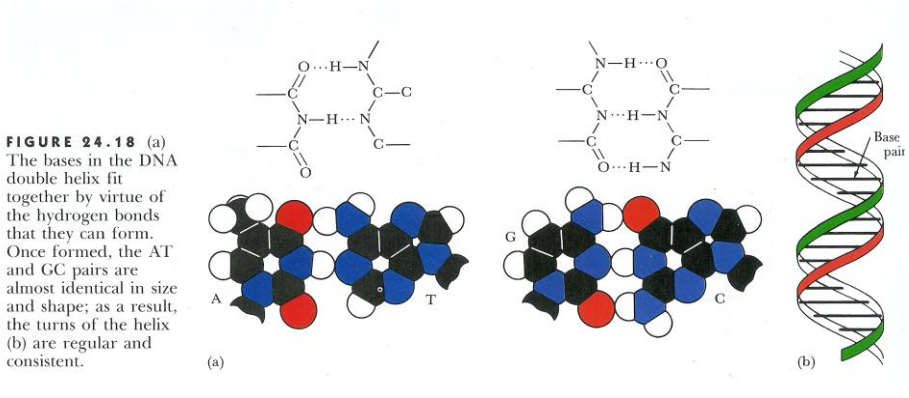

FIGURE 24.18 (a) The bases in the DNA double helix fit together by virtue of the hydrogen bonds that they can form. Once formed, the AT and GC pairs are almost identical in size and shape; as a result, the turns of the helix (b) are regular and consistent.

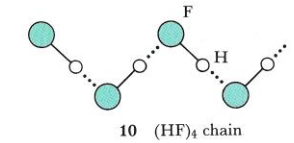

10 $(HF)_4$ chain

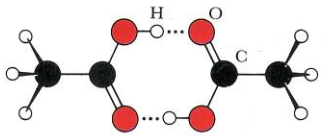

11 Acetic acid dimer

..many varieties….. widely different bond strengths

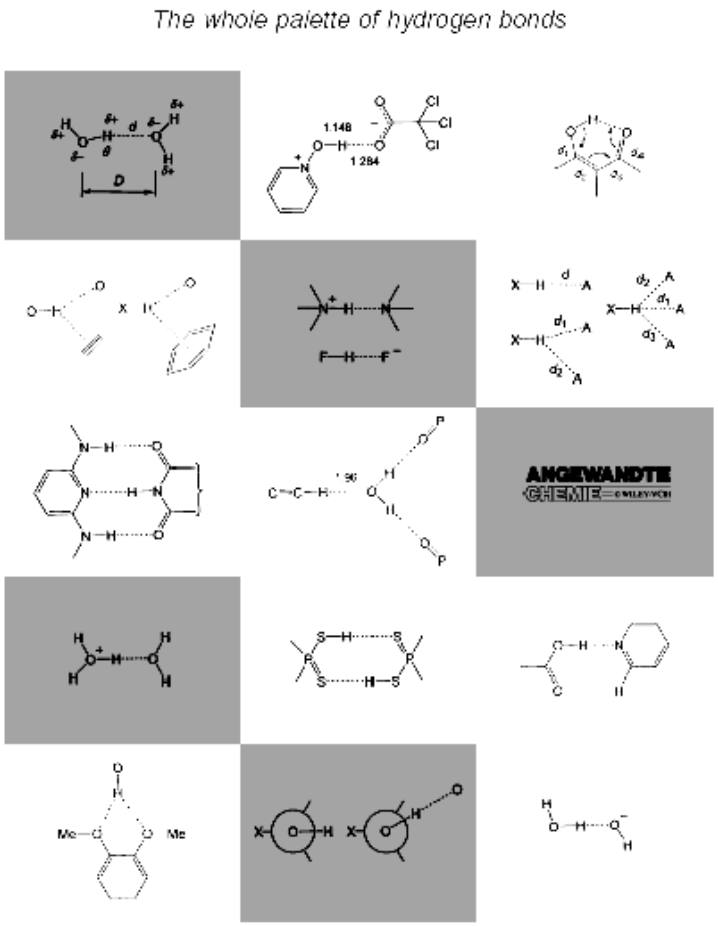

Dimer	Energy
$[F{-}H{-}F]^-$	39
$[H_2O{-}H{-}OH_2]^+$	33
$[H_3N{-}H{-}NH_3]^+$	24
$[HO{-}H{-}OH]^-$	23
$NH_4^+ \cdots OH_2$	19
$NH_4^+ \cdots Bz$	17
$HOH \cdots Cl^-$	13.5
$O{=}C{-}OH \cdots O{=}C{-}OH$	7.4
$HOH \cdots OH_2$	4.7 ; 5.0
$N{\equiv}C{-}H \cdots OH_2$	3.8
$HOH \cdots Bz$	3.2
$F_3C{-}H \cdots OH_2$	3.1
$Me{-}OH \cdots Bz$	2.8
$F_2HC{-}H \cdots OH_2$	2.1 ; 2.5
$NH_3 \cdots Bz$	2.2
$HC{\equiv}CH \cdots OH_2$	2.2
$CH_4 \cdots Bz$	1.4
$FH_2C{-}H \cdots OH_2$	1.3
$HC{\equiv}CH \cdots C{\equiv}CH^-$	1.2
$HSH \cdots SH_2$	1.1
$H_2C{=}CH_2 \cdots OH_2$	1.0
$CH_4 \cdots OH_2$	0.3 ; 0.5; 0.6 ; 0.8
$C{=}CH_2 \cdots C{=}C$	0.5
$CH_4 \cdots F{-}CH_3$	0.2

kcal mol^{-1}

T.Steiner Angew. Chemie. **41**, 48 (2002)

Investigating mechanism of bond breakage.

- Quantum state-selective **excitation** and **detection** necessary.
- System must be sufficiently complex to have potential biological relevance but be sufficiently simple that quantum state resolution is possible.
- Experiments of **Reisler et al**. on **C_2H_2 – X** species (X= HCl, DCl, NH_3) **give correlated (v;j) data i.e. energy and AM** disposal in dissociation process (H-bond breakage)

Experimental overview

1. Excite specific vibrational modes (i) **C – H *asym* stretch** of acetylene **or** (ii) **HX stretch** to initiate vibrational predissociation (VP).

2. Tunable laser 2+1 REMPI detects HCl j-states. I.r. on - i.r.off gives photofragment yield.

3. Velocity map ion images (VMI) of HCl (j=4-7) show distributions reflecting energy remaining and how disposed into C_2H_2 (v;j) states.

4.Fit translational distributions gaussians for each C_2H_2 quantum state. Energy and momentum conservation allow **unique identification of pair correlated HCl (0;j) with C_2H_2 (v;j) states.** Reisler et al PCCP **8,** 2915 (2006)

Equilibrium structures

•Dimer **equilibium** geometries determined by high-resolution spectroscopy.

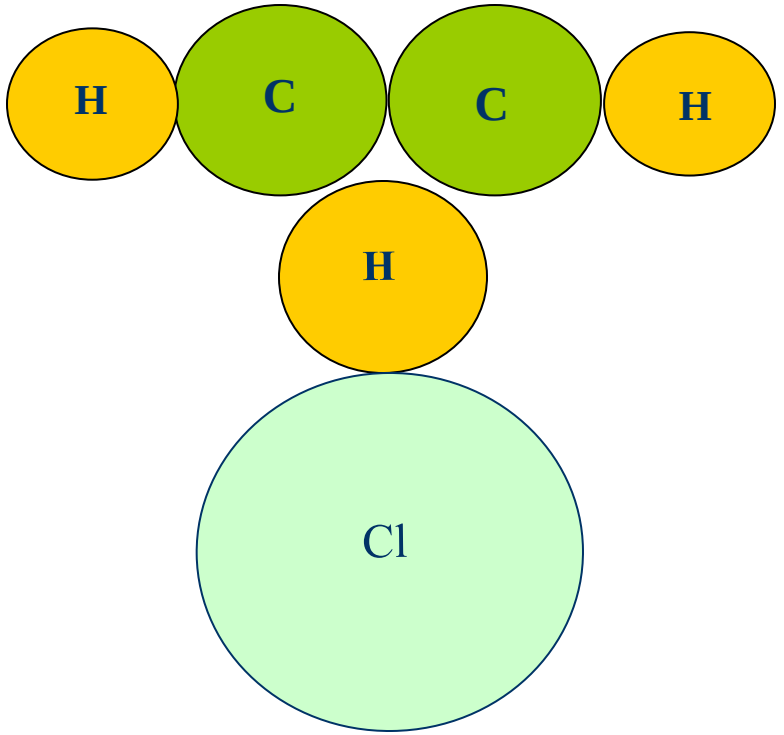

T-shaped
C_2H_2-HCl

Energy levels.

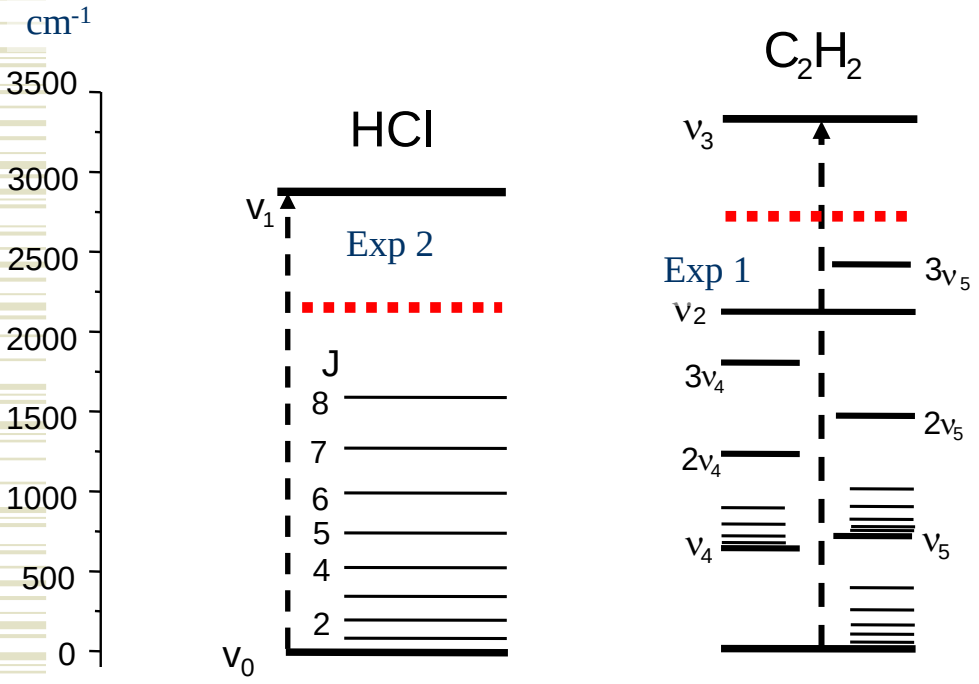

- Energy level systems linked through the H-bond

- **Each is available to accept energy and angular momentum at the moment of dissociation.**

Normal vibrations of C_2H_2

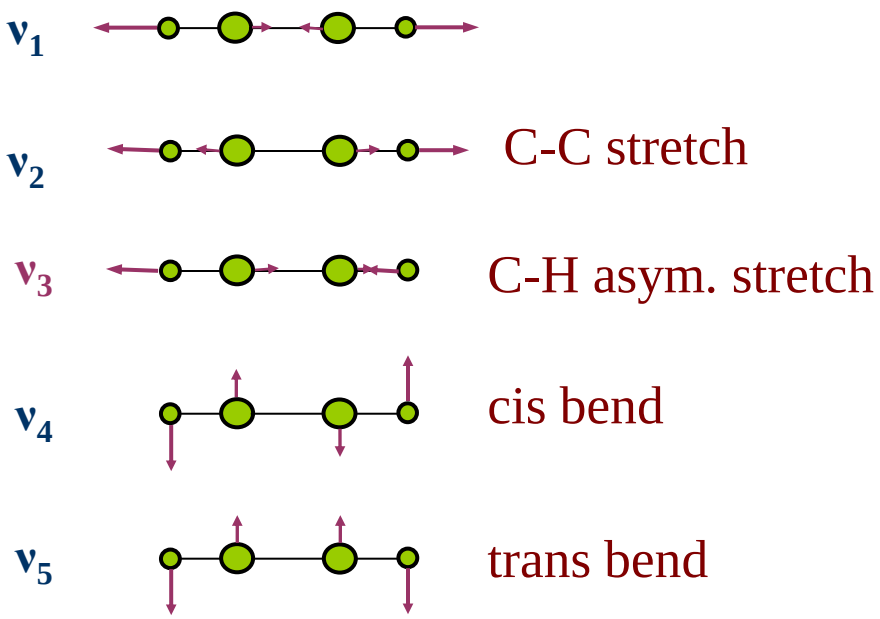

Expt. 1 initial excitation in asym stretch of complex → energy into **C-C stretch** ($\nu_{2)}$ of C_2H_2.

Expt.2 initial excitation into HCl stretch of complex → energy into **bend** modes (ν_4) and (ν_5)

In each case rotations found both in HCl and C_2H_2

Main findings

•1st step involves redistribution to |j> and/ or |v;j> states in each fragment.

• Vibrational relaxation pathways are **v.excitation mode-specific**.

• Hierarchy in distribution of energy. **Large quanta set upper limits on medium sized quanta and these set limits on smallest quanta.**

• j-values for C_2H_2 > 18 rarely observed. Direct (lowest ΔE) loss to C_2H_2 rotation never found.

Method of analysis.

• Use ‘internal collision’, angular momentum model of VP (J.C.P. **117**, 9275 (2002)). Dimer components ‘collide’ as weak bond contracts generating impulse from the vib. excitation. Impulse creates rotation and/or vibration and recoil orbital AM in departing fragments.

• Calculation treats VP as a form of (collision-induced) vibration-rotation transfer.

• Uses angular momentum (AM) model of inelastic collision (see e.g. PCCP **6**, 1637 (2004)) based on momentum conversion to calculate probability of linear-to-angular momentum change.

Linear-to-angular momentum conversion..

2. The principal **driving force** is the conversion of linear-to-(rotational) angular momentum via

$$\Delta j = \mu v_{rel} b_n$$

Δj is the change in rotational angular momentum, v_{rel} = relative velocity, μ = reduced mass, b_n is the molecular 'lever arm' converting LM→AM. In homonuclear diatomics b_n^{max} = half bond length (HBL).

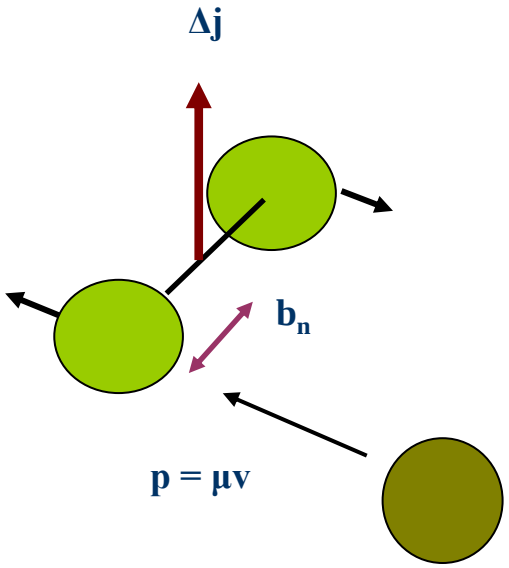

..but constrained to conserve energy

Energy conservation is maintained **for each transition** through the relationship

$$\tfrac{1}{2}\mu\, v_{rel}^{2} = \Delta E\ (=|E_f - E_i|)$$

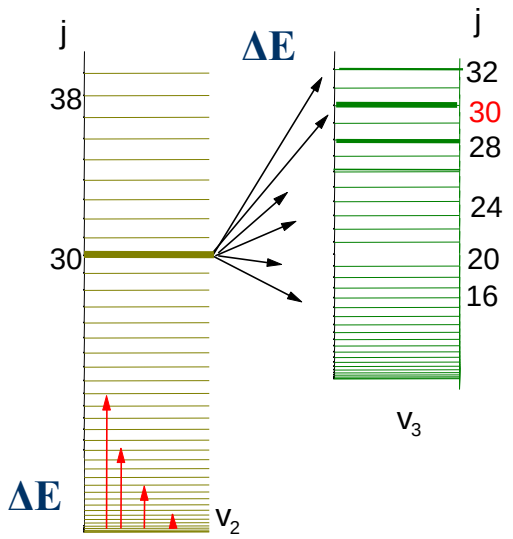

Calculating transition probabilities.

The expression for each Δj transition is

$$\Delta j = \mu\, v_{rel}\, b_n$$

The **probability** Δj occurs, P(Δj), can be written

$$\mathbf{P(\Delta j) = \mu \int_0^{v(max)} \int_0^{b(max)} P(v_{rel})\, P(b_n)\, dv_{rel}\, db_n}$$

$P(v_{rel})$ the velocity distribn. is usually known.
$P(b_n)$ is evaluated from experiment (exp. decay in which $\mathbf{b_n^{max} = HBL.}$)

Quantitative calculations

A **quantitative** method uses a hard shape model of the molecule based on molecular dimensions. For a diatomic molecule, this is a 3D ellipsoid for which A-B = HBL (A & B are semi-major and semi-minor ellipse axes).

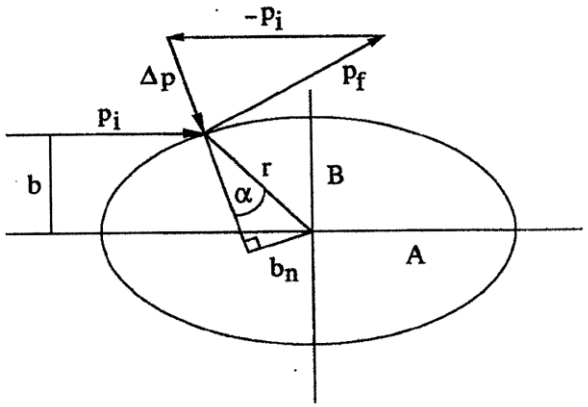

The ellipsoid dynamics have been incorporated into a program with Monte-Carlo generated random collision trajectories (typically 20 x 10^6) for each interaction.

Testing the model; OH-X weakly bound complexes

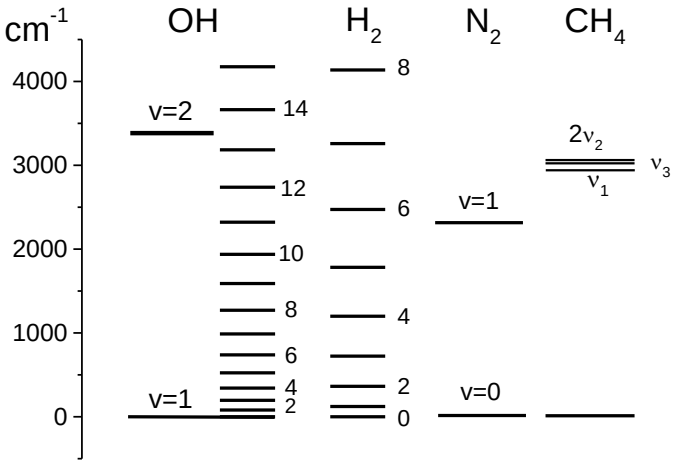

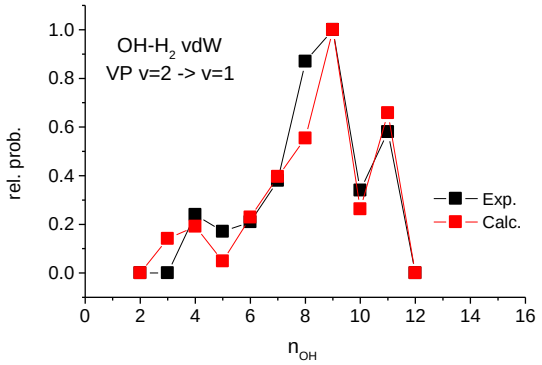

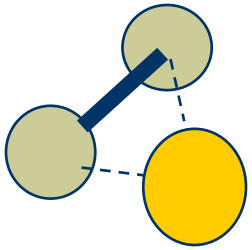

Calculations reproduce rotational distributions in OH-X complexes if we assume energy loss into rotation or vibration of X. (JPC A **109**, 5005 (2005)

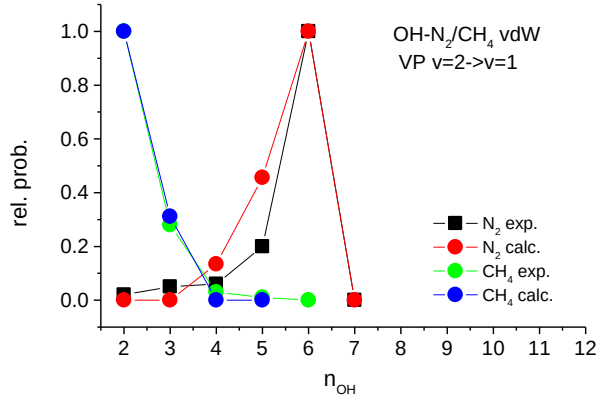

Calculations

Dissociation geometry is restricted by relative motion of component species so that $\mathbf{b_n^{max} < HBL}$ Vary b_n^{max} to fit data. **Best fit values give relative geometry of partners at moment of dissociation**.

First calculate rotation distribution in HCl caused by 'collision' with C_2H_2. Then calculate rotations in C_2H_2 caused by 'collision' with HCl **for each j** value of HCl. Depending on excitation method, one of these represents **rotational transfer (RT),** the other **vibration-rotation transfer (VRT)**

C-H asym stretch excitation: **HCl rotation**.

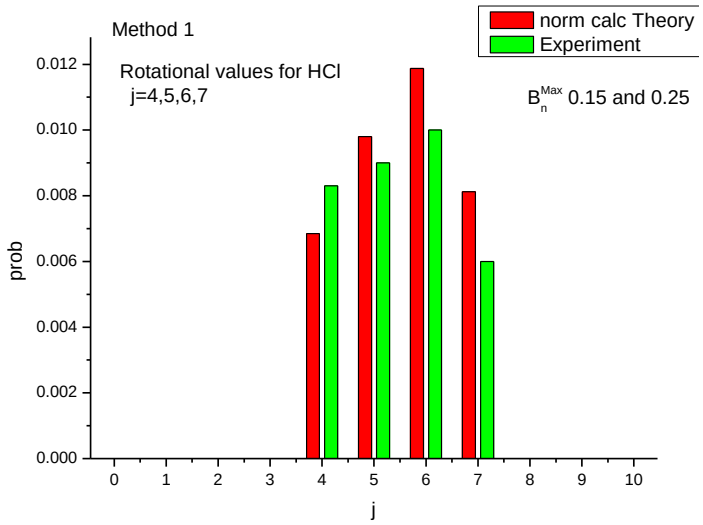

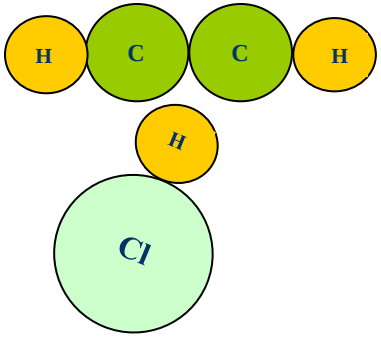

Calculated (red) and experimental (green) HCl rotational distributions following C_2H_2 asym. stretch excitation. b_n^{max} = 0.15 and 0.25 Å i.e. **very small tilt of HCl relative to c.m.**

C-H asym stretch excitation: C_2H_2 rotation.

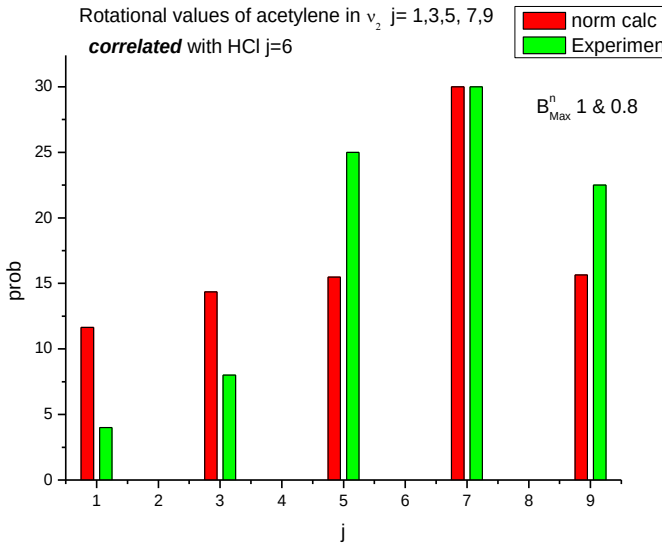

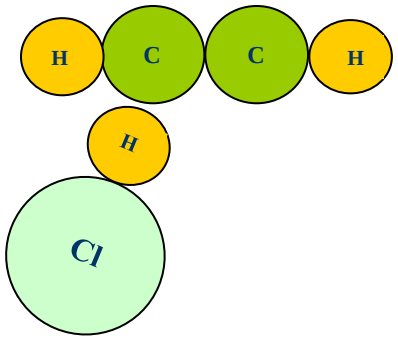

Rotational distribution in ν_2 (C-C stretch) of C_2H_2 **correlated with j = 6 of HCl** following excitation of ν_3 (C-H antisym. stretch) of C_2H_2. Green bars show experimental data, red are calculated values using b_n^{max} = 1.0 and 0.8 Å.

C-H asym stretch excitation: C_2H_2 rotations.

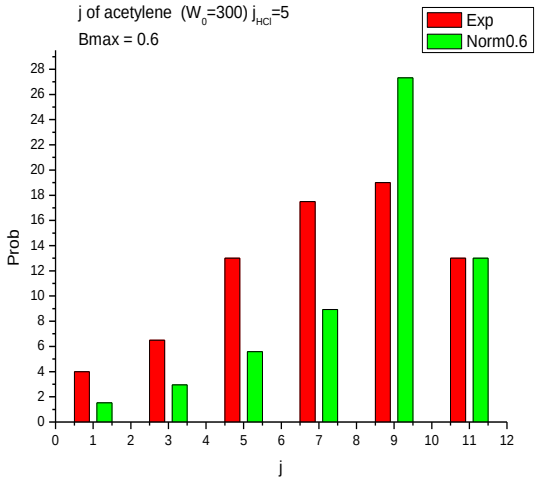

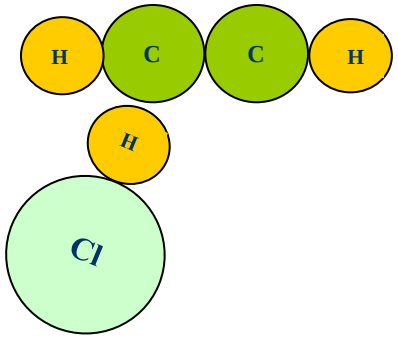

Rotational distribution in ν_2 (C-C stretch) of C_2H_2 **correlated with j = 5 of HCl** following excitation of ν_3 (C-H antisym. stretch) of C_2H_2. Red bars show experimental data, green are calculated values using $b_n^{max} = 0.6$ Å.

HCl stretch excitation: **HCl rotations**.

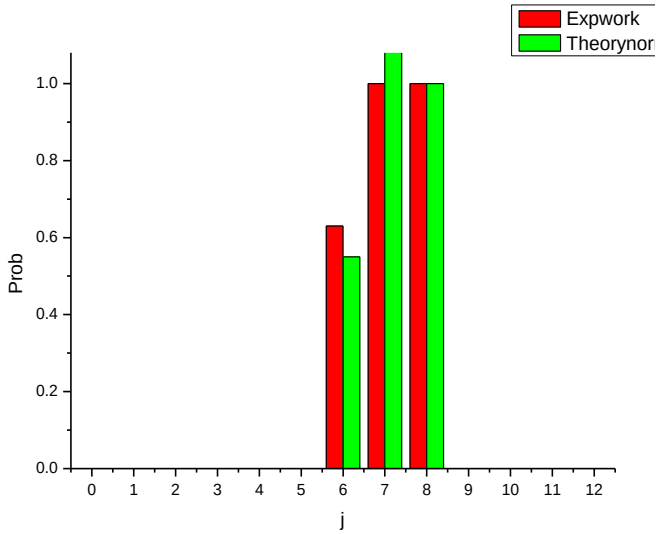

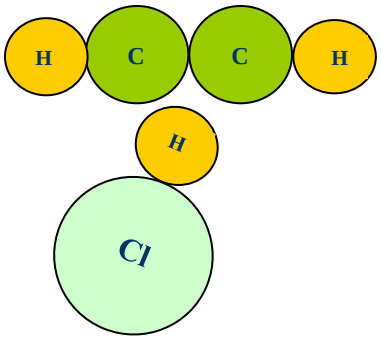

Calculated (green) and experimental (red) HCl rotational distributions following HCl excitation. b_n^{max} = 0.2 and 0.26 Å

What the results tell us (i)

1. No dissociation from equilibrium geometry.

2.Model based on (**nuclear**) momentum change in molecules having shape and size familiar throughout chemistry reproduces these very detailed and precise experiments with good accuracy.

3.Except for **quantisation** in molecules, results are just **what we would expect from behaviour of macroscopic objects**. Motion on a complex PES not required.

4.Dissociation requires internal impact at **specific relative configurations that change vibrational motion and simultaneously excite rotation**.

What the results tell us (ii).

5. Excitation appears to remain **localised within the mode** initially excited until the moment of dissociation. No rapid intramolecular redistribution.

A very localised perturbation (the internal collision) initiates the dissociation. **Acceptable exit routes must meet demands of simultaneous energy and angular momentum conservation**. **Suggests that requirements of product states set the conditions for 'successful' dissociation.**

Can we predict dissociation routes?

- **In principle, yes**. VP involves RT in one fragment and VRT the other. Can calculate probability of each and convolute to get a joint probability of the two events (see figure).

- **In practice? (a)** Many potential fragment states to sum over e.g. **4000 in acetylene HF dimer**.

(b) Many routes - must demonstrate some have low some high probability

(c) v. different patterns exist within the acetylene – HX series.

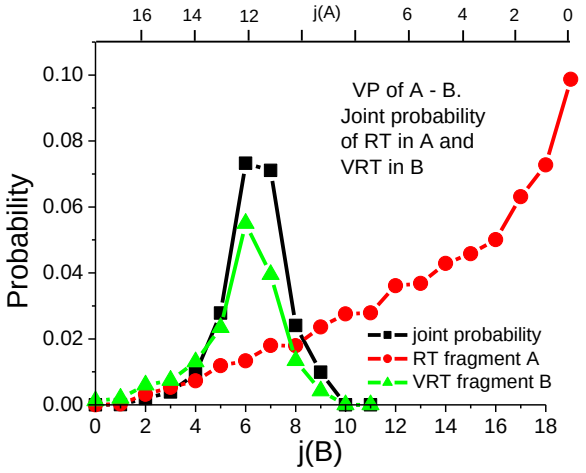

Results: C_2H_2 – HCl: HCl distributions

Upper graph: C – H asym stretch excitation. **Lower graph**: HCl stretch excitation. (*Note: experiment unable to measure probability for j(HCl) < 4*).

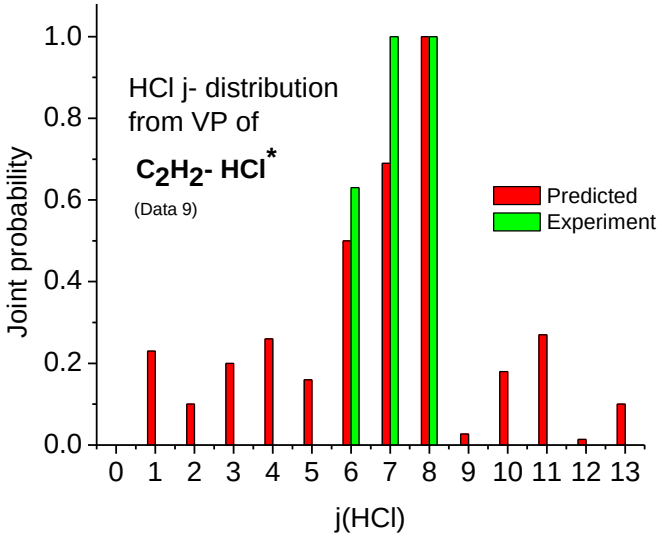

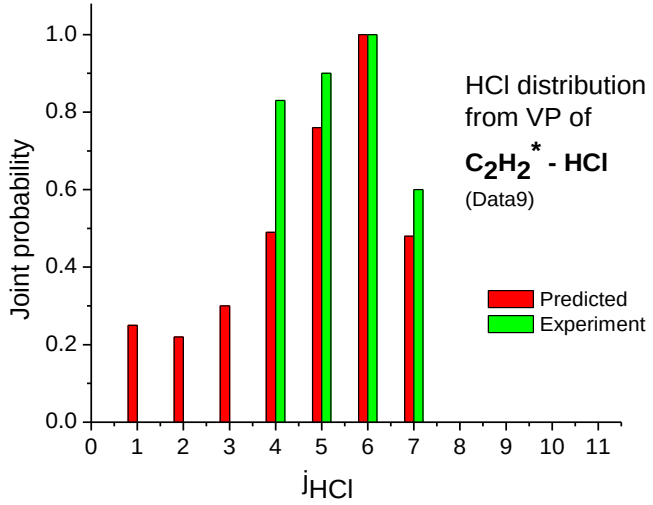

2. C_2H_2 – HX (X=O,F). HX stretch excitation

VP of these involves HX rotation (up to maximum accessible) plus acetylene rotation (HF) or vibration-rotation (OH)

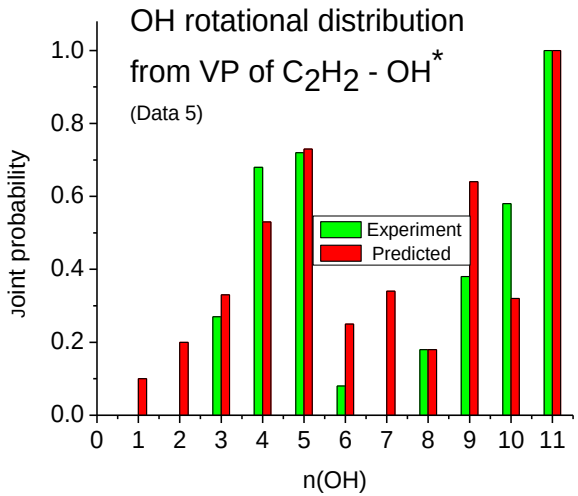

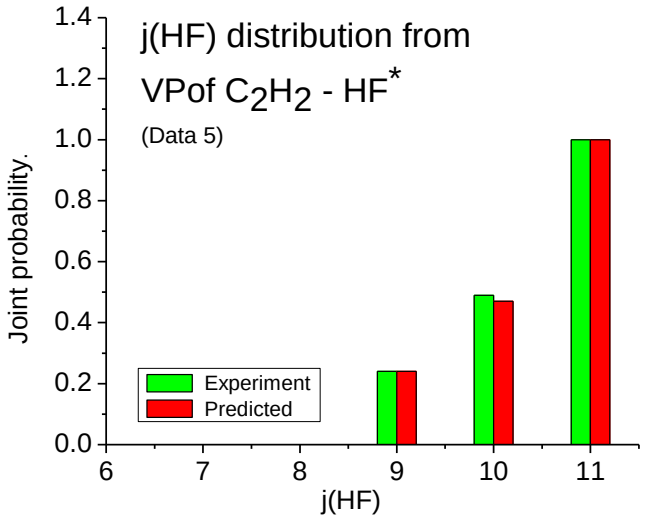

Some general principles

1. The fragment v-states accessed are determined primarily by the **initial impact direction**.
2. Dissociation routes that require j(C_2H_2) > 20 highly improbable.
3. Initial impulse must be able to excite simultaneously the destination **vibration AND rotations** about an inertial axis.
4. The nuclear dynamics of state-to-state momentum inter-conversion within a framework of energy (and AM) conservation provides understanding of the VP event

Acknowledgements

Experimental: **Hanna Reisler, Jessica Parr**;
Chemistry Department, USC Los Angeles.

Calculations: **Marisian Pritchard**,
Chemistry Dept. University of Sussex

Interrogating the fragments: HCl

HCl v=0 rotational state populations determined by resonance-enhanced multi-photon ionisation (REMPI). Find that j = 4, 5, 6, 7 only are appreciably populated.

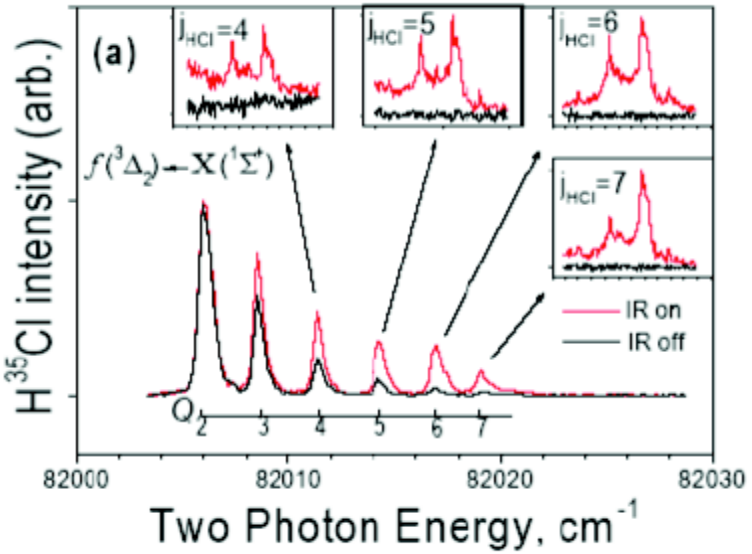

Acetylene-HCl: HCl distributions.

Expt.1 C_2H_2 (ν_3) excitation

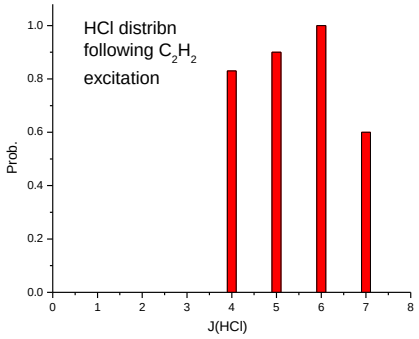

Expt.2 HCl excitation

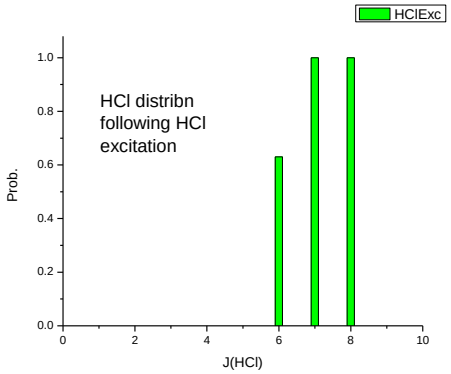

Indicate a constrained dissociation geometry

Acetylene fragment translational energies.

Acetylene fragments **correlated with specific HCl rotational states** are analysed using velocity-map ion imaging (VMI). The acetylene velocities are transformed to acetylene (v;j)- state populations.

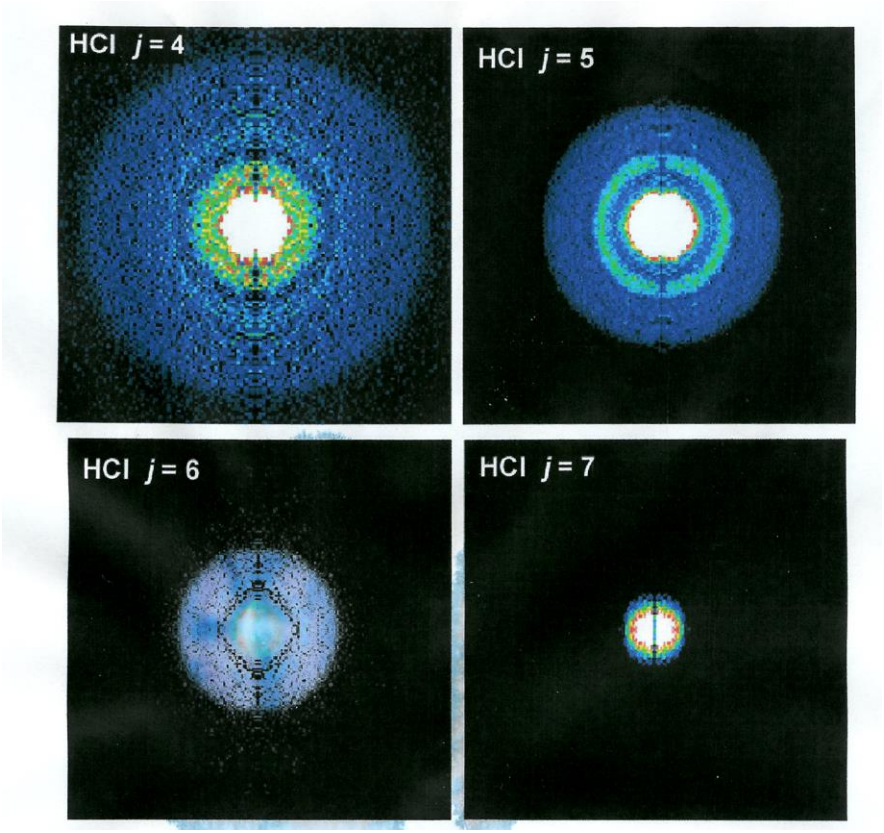

Acetylene rotation state populations

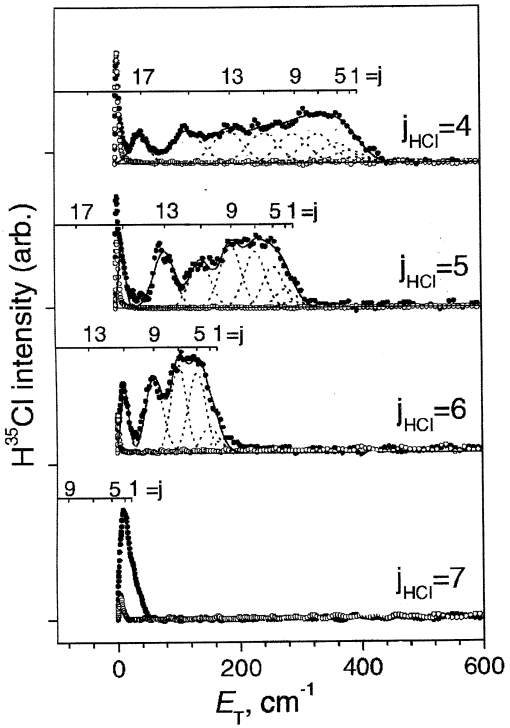

Fig. 4 Center-of-mass (c.m.) translational energy (E_T) distributions corresponding to images of HCl(j = 4–7) shown in Fig. 3. The odd j assignments correspond to rotational states of the acetylene co-fragment produced with one quantum in ν_2 (C–C stretch mode). See the text for details.

Expt.1 Excite C_2 H_2 asym stretch. Only C-C sym. stretch (ν_2) populated

Expt.2 Excite HCl stretch. Only bend modes (ν_4 and ν_5) populated.

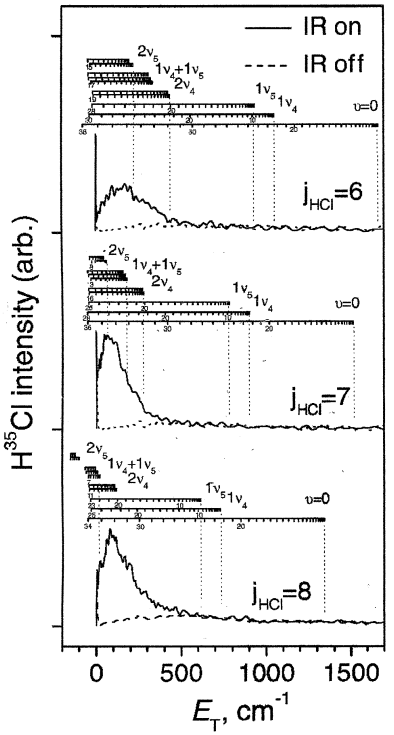

Fig. 6 C.m. translational energy distributions obtained by pumping the Q band of the HCl stretch of the dimer at 2806.9 cm^{-1} and recording images of HCl(j = 6–8). The dashed vertical lines indicate the translational energy thresholds for vibrational modes of the acetylene co-fragment assuming D_0 = 700 cm^{-1}. The sticks indicate the rotational states of each vibrational mode of the acetylene co-fragment; the numbers under the bars give the rotational state assignments. Both odd and even j can be populated, as explained in the text.

C_2H_2 -HCl: acetylene distributions

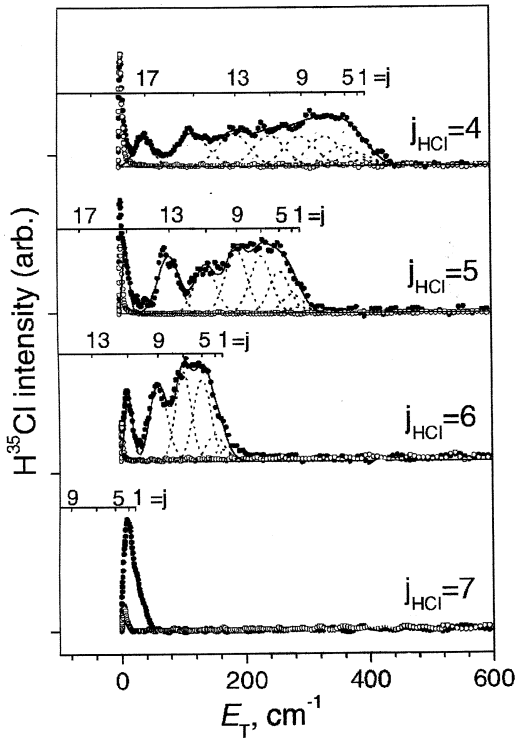

Fig. 4 Center-of-mass (c.m.) translational energy (E_T) distributions corresponding to images of HCl(j = 4–7) shown in Fig. 3. The odd j assignments correspond to rotational states of the acetylene co-fragment produced with one quantum in ν_2 (C–C stretch mode). See the text for details.

Expt.1 C_2H_2 asym. stretch exc. C-C sym. stretch (ν_2) populated only.

Expt.2 HCl exc. Bend modes (ν_4 and ν_5) populated only.

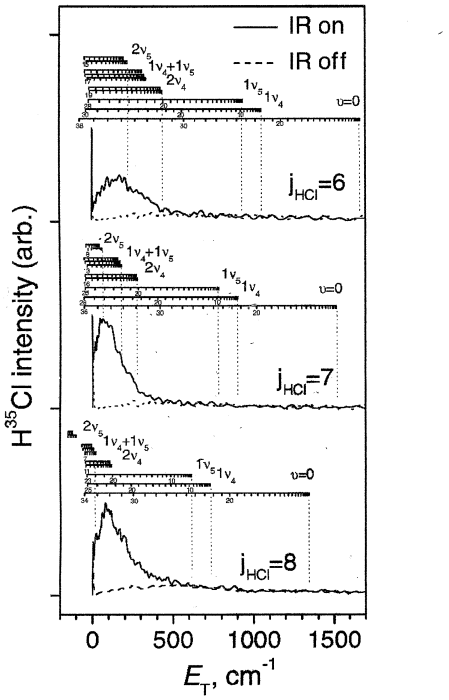

Fig. 6 C.m. translational energy distributions obtained by pumping the Q band of the HCl stretch of the dimer at 2806.9 cm^{-1} and recording images of HCl(j = 6–8). The dashed vertical lines indicate the translational energy thresholds for vibrational modes of the acetylene co-fragment assuming D_0 = 700 cm^{-1}. The sticks indicate the rotational states of each vibrational mode of the acetylene co-fragment; the numbers under the bars give the rotational state assignments. Both odd and even j can be populated, as explained in the text.

C_2H_2 – NH_3 experiment.

NH_3 – only the ‘umbrella mode excited plus v small amount of rotation.

C_2H_2 – Now the ν_2 mode (C-C stretch) is not energetically accessible. Only bend modes (ν_4 and ν_5) are available. Rotational distributions suggest NH_3 makes impact in two locations one of which is well away from the end of the ellipsoid and close to the C-atom.

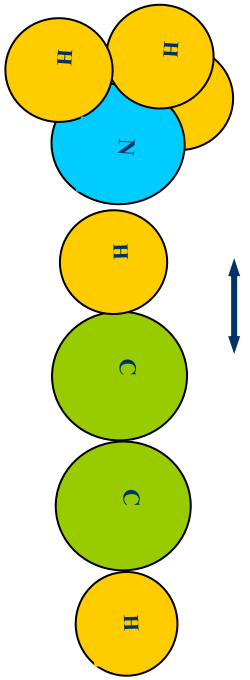

Findings

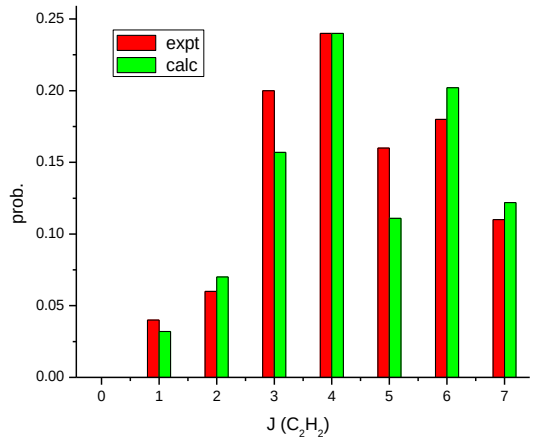

Fig. X1 Calculated (red columns) and experimental (green columns) rotational distributions in the ***v_4 mode of C_2H_2*** *coincident with* $2v_2^+$*;* ${}^rR_0(1)$ *of* NH_3*. Two values of* b_n^{max} *were used to fit the data, namely* ***0.64*** *and* ***1.2Å***

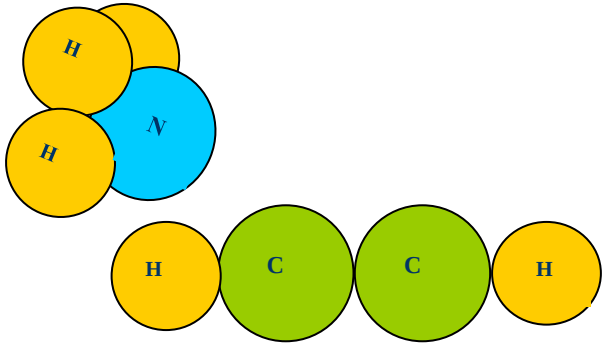

Wide amplitude motion about the H-end of acetylene

N atom is hit on a line very close to its centre of mass.

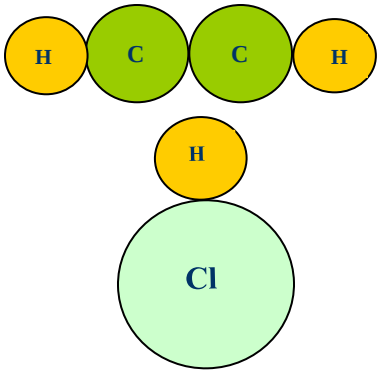
H
C
C
H
H
Cl

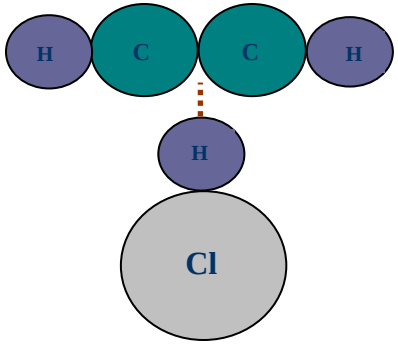
H
C
C
H
H
Cl

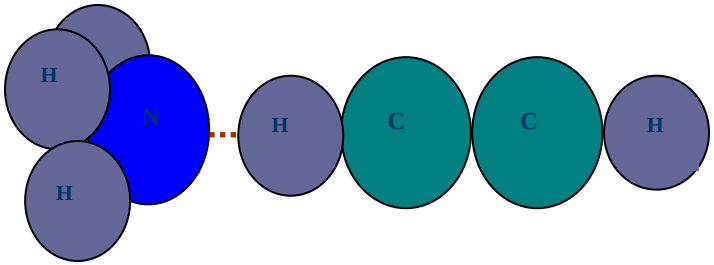
H
N
H
H
C
C
H

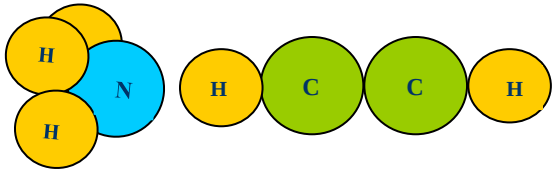
H
N
H
H
C
C
H

The experiment – diatomics

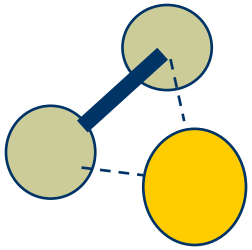

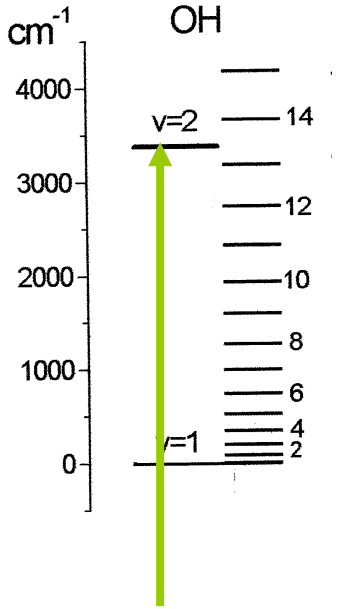

Excite chemical bond with laser. Some time later vibrational predissociation (VP) occurs

Experimental observables:

1. rotational distribution.

2. translational energy release

3. VP lifetime.

Calculating rotational distributions.

1. Assume VP is analogous to collision-induced vibration-rotation transfer, i.e. dissociation results from an 'internal' collision.

2. Use angular momentum (AM) method * to calculate probability of generating molecular rotation from the energy available on dissociation.

* See e.g. PCCP **6**, 1637 (2004) for recent review

Experimental data (Lester et al.) and results of calculations: OH-X

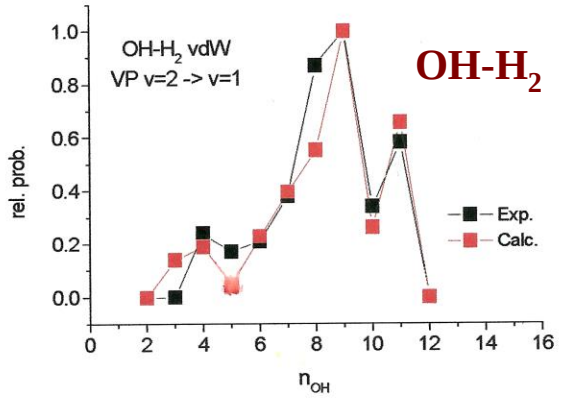

OH-CH_4

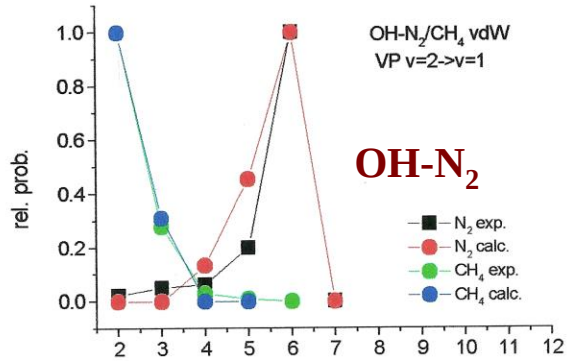

Calculations allow for energy take-up into rotation and/ or vibration of the partner species e.g. rotations 0-2,4,6; 1-3,5,7 in H_2 and vibrational excitation in N_2 and CH_4

(See J.Chem. Phys. **117**, 9275 (2002))

Polyatomics are trickier…

1. Rotations take place about more than one axis → J- and/or K-changing transitions.

2. Rotational structure difficult to resolve.

3. Distribution *shape* (peak and J(max)) can still be very informative on dissoc. dynamics.

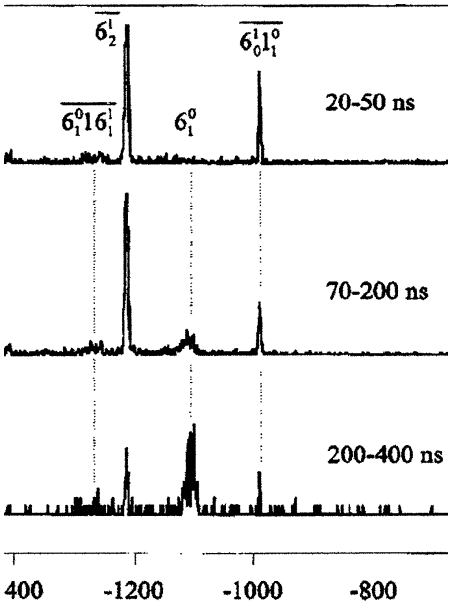

Benzene-Ar. Dissoc. from 6^1 is slow & signal v. weak.

VP of benzene-Ar $6^1 \rightarrow 0^0$

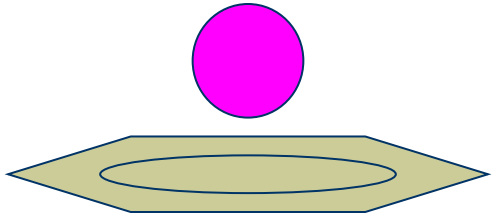

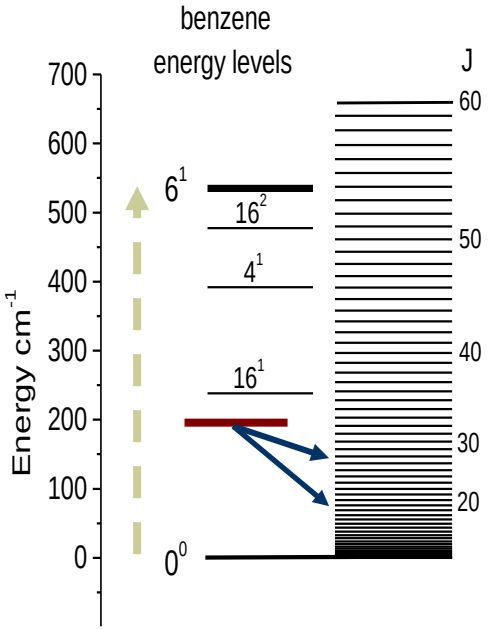

Benzene-Ar energetics

E_{vib}	522 cm^{-1}
E_{vdW}	335 cm^{-1}
E_{avail}	187 cm^{-1}

Method of calculation: the equivalent rotor

- **Build on successful model for collisional transfer in diatomics**.

- **For J- or K-changing processes.**
'Equivalent rotor' - linear rotor having mom. of inertia, bond length and rot. constant of polyatomic along inertial axis of interest, i.e. that giving rise to J- or K-transition.

- **Dimensions of equiv. rotor determined by shape, size and mass distribn. of polyatomic.**

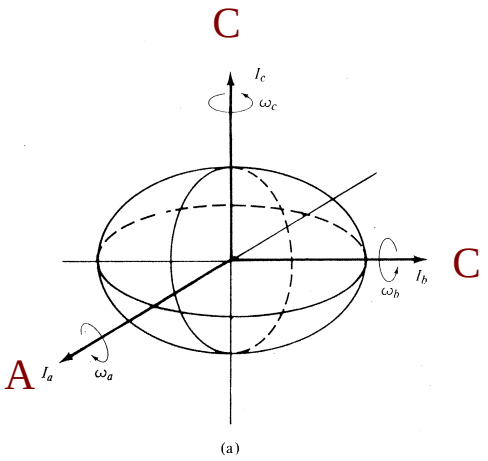

Oblate

$I_A \sim I_B < I_C$

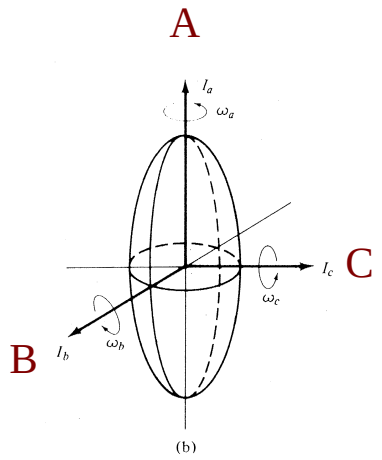

Prolate

$I_A < I_B \sim I_C$

Testing the equivalent rotor model

Few state-to-state RT and VRT data sets available. Most extensive are

(1) glyoxal-Ne (Parmenter)

(2) C_2H_2 – He (Smith)

(3) C_6H_6 – H_2 (Lawrance) from lineshape fit.

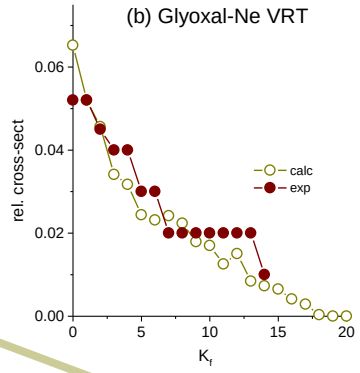

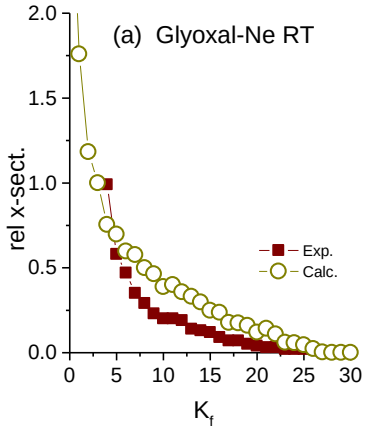

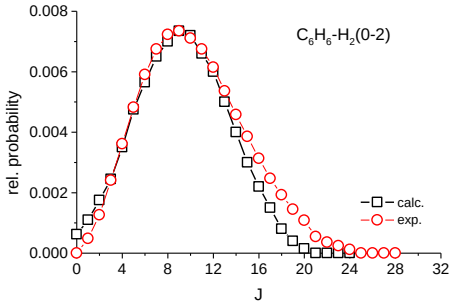

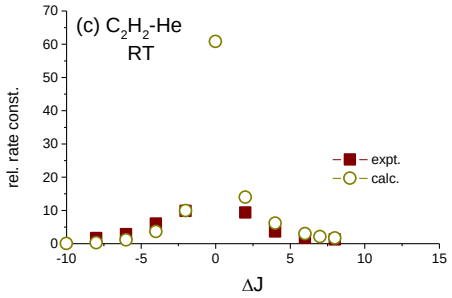

Equivalent rotor method works well for each of these. (J.Chem. Phys. 121, 169 (2004)

Benzene-Ar VP: experimental data

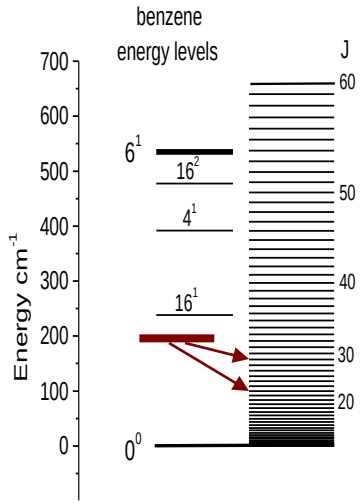

Dissociated products detected by velocity map imaging (VMI) and dispersed fluorescence.

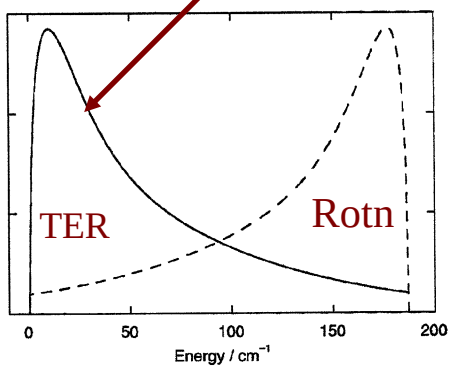

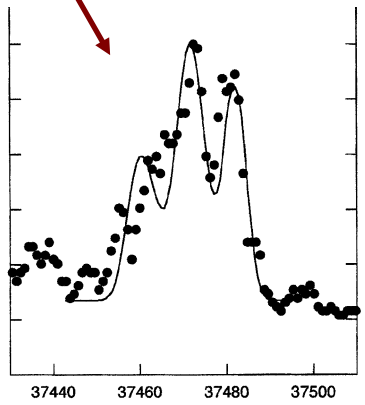

TER data gives rotational distribution and dispersed fluorescence lineshape gives gives proportion of J- and K-excitation.

Almost entirely J-changing

Comparison between theory and experiment

An unknown is the point in the overall benzene-Ar motion where dissociation occurs. This distance (b_n^{max})varied for best fit. Peak depends on J_i - also varied. JCP **122**, 074311 (2005)

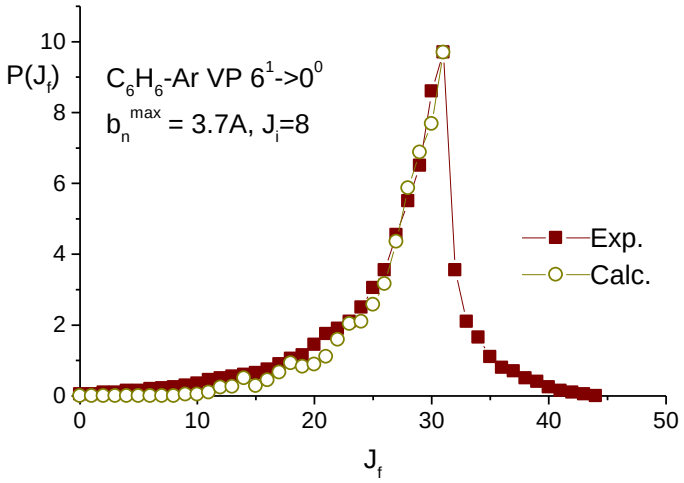

Best fit values

J_i = 8±1 (exp=7)

b_n^{max} = 3.7±0.1Å

Dissociation occurs from edge of ring

Spectroscopic evidence for bound orbiting states following ivr $6^1 \rightarrow 16^1$ CPL **401**, 440 (2005)

p-difluorobenzene-Ar ; s-tetrazine-Ar

Data for these much less precise. Estimates of peak JK and max values made from dispersed fluorescence.

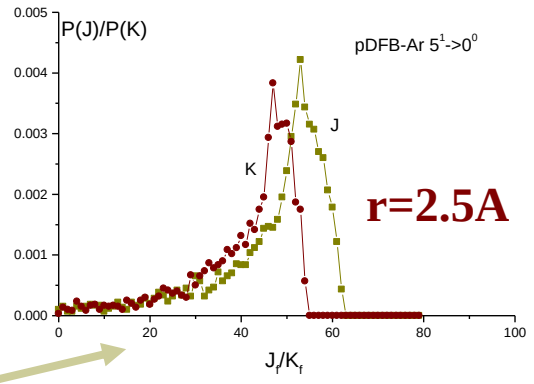

Experimental data

p-DFB $J_{peak} \sim K_{peak} = 45\text{-}50$

s-tetrazine $J_{peak} \sim 15$; $J_{max} \sim 25$

Calculations

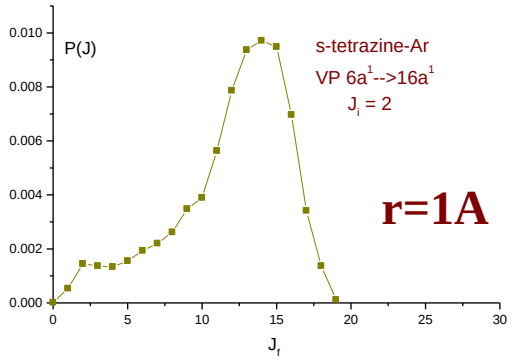

Summary

- As in the case of diatomics the dissociation consists of vibration-to-rotation conversion.
- Results suggest that dissociation is efficient when the vibrational mode is able to generate rotation about an inertial axis.
- Equivalent rotor calculations give an estimate of the rotational distribution when this is not known and can be used to evaluate the dissociation geometry when this distribution is measured.
- Dissociation from 6^1 of benzene-Ar is slow and other processes compete.
- **More rotational distribution measurements needed!**